

Spin polarization and color superconductivity in the Nambu-Jona-Lasinio model at finite temperature

Hiroaki Matsuoka*

Graduate School of Integrated Arts and Science, Kochi University, Kochi 780-8520, Japan

Yasuhiko Tsue†

Physics Division, Faculty of Science, Kochi University, Kochi 780-8520, Japan

João da Providência and Constança Providência

CFisUC, Departamento de Física, Universidade de Coimbra, 3004-516 Coimbra, Portugal

Masatoshi Yamamura

Department of Pure and Applied Physics, Faculty of Engineering Science, Kansai University, Suita 564-8680, Japan

(Dated: November 9, 2016)

We investigate the possible existence of spin polarization and color superconductivity in the Nambu-Jona-Lasinio model with a tensor-type interaction at finite density and temperature. The thermodynamic potential is calculated by the functional integral method. Numerical results indicate that at low temperature and quark chemical potential the chiral condensed phase exists, and at intermediate chemical potential the color superconducting phase appears. In addition, depending on the magnitude of the tensor coupling, at large chemical potential and low temperature, a color superconducting phase and a spin polarized phase may coexist while at intermediate temperatures only the spin polarized phase occurs.

PACS numbers: 21.65.Qr, 12.39.Fe

I. INTRODUCTION

One of the most interesting topics in high energy physics is to clarify the phase structure of quantum chromodynamics (QCD). The phase where we live is called hadronic phase. A remarkable feature in this phase is that quarks and gluons are confined. At high temperature, quark-gluon plasma (QGP) phase is realized. Quarks and gluons are not confined in the QGP phase. This phase has been confirmed by high energy accelerator experiments, for example, the relativistic heavy ion collider (RHIC) experiment. Moreover, more powerful experiments have been conducted by the large hadron collider (LHC).

On the other hand, the phase structure at low temperature and large chemical potential has not been understood very well. Since presently, it is still not possible to test the low temperature and large chemical potential regime in the laboratory, and we cannot use the lattice simulation method because of the “sign problem”, the features of this region of the QCD phase diagram are still uncertain. In order to investigate the nature at such conditions the Nambu-Jona-Lasinio (NJL) model [1, 2] has been used. It has been considered that a color superconducting phase [3–5], which may occur in different forms such as the two-flavor color superconducting (2SC) phase or the color flavor-locked (CFL) phase, may be realized

under these conditions. This phase may appear inside compact stars, such as neutron stars. Compact stars are very dense astrophysical objects which may have very strong magnetic fields [6]. However, the mechanism that explains the generation of such strong magnetic fields is still not completely understood. In particular, the phase structure at large chemical potential and the possible existence of a spin polarized phase should be investigated.

The possible existence of a quark ferromagnetic phase has been discussed with one-gluon-exchange interaction in Ref.[7]. Moreover, the possibility that spins of quarks may polarize at large chemical potential has been studied with axial vector-type interaction in Refs. [7–10]. In Ref.[11], a vector-type interaction which respects chiral symmetry has been introduced in the NJL model and it has been shown that spin polarization could occur if the chemical potential is within a narrow range of values. The relationship between the vector-type interaction and the 2SC has been discussed and it has been indicated that chiral condensed phase and 2SC phase may coexist if the contribution from the vector-type interactions considered in Ref.[12].

Although a term for spin polarization can be derived from the vector-type interaction, we pay attention to a tensor-type interaction, which, of course, respects chiral symmetry. The interaction has been introduced in Ref.[13] and a spin polarization term can be derived from it. Note that the spin polarization term from the tensor-type interaction is not identical to that from the vector-type interaction, and the term from the tensor-type interaction can be interpreted as an anomalous magnetic moment induced dynamically according to Ref.[14]. In

* b16d6a01@s.kochi-u.ac.jp

† tsue@kochi-u.ac.jp

Refs.[15, 16] the relationship between the spin polarization and the color superconductivity has been investigated at zero temperature, and in our preceding paper [17] the discussion has been extended to finite temperature. According to our preceding paper, the chiral condensed phase and the spin polarized phase do not coexist, and the order of the phase transition from the spin not-polarized phase to the spin polarized phase is second order. The effect from an external magnetic field on the spin polarization has been studied in Ref.[18], and it has been shown that ferromagnetism may occur if we assume an anomalous magnetic moment for the quarks. In the present work, we investigate the possible existence of spin polarization and color superconductivity in the Nambu-Jona-Lasinio model with a tensor-type interaction at finite density and temperature.

In the following section we introduce the NJL model with the tensor-type interaction and calculate the thermodynamic potential by the functional integral method. In section III we evaluate the thermodynamic potential numerically. The last section is devoted to the conclusions and remarks. The tensor-type interaction can be derived from the scalar-interaction channel in the NJL model, however, we treat the coupling constant for the tensor-type interaction as a free parameter. We use the gamma matrices in the Dirac representation, and adopt the metric tensor: $g^{\mu\nu} = \text{diag}(1, -1, -1, -1)$.

II. NJL MODEL WITH TENSOR-TYPE INTERACTION AND QUARK PAIRING INTERACTION

We start from the NJL model with the tensor-type interaction and quark pairing interaction at finite quark chemical potential μ . The Lagrangian density with flavor $SU(2)$ and color $SU(3)$ symmetry at chiral limit can be expressed as

$$\begin{aligned}\mathcal{L}_{\text{total}} &= \mathcal{L}_{\text{NJL}} + \mathcal{L}_T + \mathcal{L}_C + \mu\bar{\psi}\gamma^0\psi, \\ \mathcal{L}_{\text{NJL}} &= \bar{\psi}i\gamma^\mu\partial_\mu\psi + G_S\{(\bar{\psi}\psi)^2 + (\bar{\psi}i\gamma^5\vec{\tau}\psi)^2\}, \\ \mathcal{L}_T &= -\frac{G_T}{4}\left\{(\bar{\psi}\gamma^\mu\gamma^\nu\vec{\tau}\psi) \cdot (\bar{\psi}\gamma_\mu\gamma_\nu\vec{\tau}\psi) \right. \\ &\quad \left. + (\bar{\psi}i\gamma^5\gamma^\mu\gamma^\nu\psi)(\bar{\psi}i\gamma^5\gamma_\mu\gamma_\nu\psi)\right\}, \\ \mathcal{L}_C &= \frac{G_C}{2}\sum_{A=2,5,7}\left\{(\bar{\psi}i\gamma^5\tau_y\lambda_A\psi^C)(\bar{\psi}^Ci\gamma^5\tau_y\lambda_A\psi) \right. \\ &\quad \left. + (\bar{\psi}\tau_y\lambda_A\psi^C)(\bar{\psi}^C\tau_y\lambda_A\psi)\right\},\end{aligned}$$

where τ_i ($i = x, y, z$) is Pauli matrix for flavor space and λ_A ($A = 2, 5, 7$) is Gell-Mann matrix for color space. The superscript C means charge conjugate. Note that \mathcal{L}_T and \mathcal{L}_C are the tensor-type interaction term and the quark pairing interaction term, respectively. In order to study the system at finite density, we introduce quark chemical potential μ . Here we use the same value for the quark chemical potential for up- and down-quarks. The spin

polarization term appears from \mathcal{L}_T when $\mu = 1$, $\nu = 2$ or $\mu = 2$, $\nu = 1$ as follows:

$$\Sigma_z = -i\gamma^1\gamma^2 = \begin{pmatrix} \sigma_z & 0 \\ 0 & \sigma_z \end{pmatrix},$$

where σ_z is the third component of Pauli matrices.

Since we ignore the collective excitations on the realized vacuum in this paper, the Lagrangian density that we consider here is as follows:

$$\begin{aligned}\mathcal{L} &= \bar{\psi}i\gamma^\mu\partial_\mu\psi + G_S(\bar{\psi}\psi)^2 + \frac{G_T}{2}(\bar{\psi}\Sigma_z\tau_z\psi)^2 \\ &\quad - \frac{G_C}{2}(\bar{\psi}\gamma^5\tau_y\lambda_2\psi^C)(\bar{\psi}^C\gamma^5\tau_y\lambda_2\psi) + \mu\bar{\psi}\gamma^0\psi.\end{aligned}\quad (1)$$

We will calculate the thermodynamic potential by the functional integral method. Let us introduce the generating functional Z :

$$\begin{aligned}Z &\propto \int \mathcal{D}\bar{\psi}\mathcal{D}\psi \exp\left[i\int d^4x\left\{\bar{\psi}i\gamma^\mu\partial_\mu\psi + G_S(\bar{\psi}\psi)^2 \right. \right. \\ &\quad \left. \left. + \frac{G_T}{2}(\bar{\psi}\Sigma_z\tau_z\psi)^2 - \frac{G_C}{2}(\bar{\psi}\gamma^5\tau_y\lambda_2\psi^C)(\bar{\psi}^C\gamma^5\tau_y\lambda_2\psi) \right. \right. \\ &\quad \left. \left. + \mu\bar{\psi}\gamma^0\psi\right\}\right].\end{aligned}\quad (2)$$

We introduce auxiliary fields in order to perform functional integral with respect to quark fields. The auxiliary fields that we introduce here are as follows:

$$\begin{aligned}1 &= \int \mathcal{D}M \exp\left[-i\int d^4x\left\{M/2 + G_S(\bar{\psi}\psi)\right\} \right. \\ &\quad \left. \times G_S^{-1}\left\{M/2 + G_S(\bar{\psi}\psi)\right\}\right], \\ 1 &= \int \mathcal{D}F \exp\left[-\frac{i}{2}\int d^4x\left\{F + G_T(\bar{\psi}\Sigma_z\tau_z\psi)\right\} \right. \\ &\quad \left. \times G_T^{-1}\left\{F + G_T(\bar{\psi}\Sigma_z\tau_z\psi)\right\}\right], \\ 1 &= \int \mathcal{D}\Delta^\dagger\mathcal{D}\Delta \exp\left[-\frac{i}{2}\int d^4x\left\{\Delta^\dagger + G_C(\bar{\psi}^C\gamma^5\tau_y\lambda_2\psi)^\dagger\right\} \right. \\ &\quad \left. \times G_C^{-1}\left\{\Delta + G_C(\bar{\psi}^C\gamma^5\tau_y\lambda_2\psi)\right\}\right] \\ &= \int \mathcal{D}\Delta^\dagger\mathcal{D}\Delta \exp\left[-\frac{i}{2}\int d^4x\left\{\Delta^\dagger - G_C(\bar{\psi}\gamma^5\tau_y\lambda_2\psi^C)\right\} \right. \\ &\quad \left. \times G_C^{-1}\left\{\Delta + G_C(\bar{\psi}^C\gamma^5\tau_y\lambda_2\psi)\right\}\right].\end{aligned}$$

Inserting the above auxiliary fields into the generating functional, we obtain

$$\begin{aligned}Z &\propto \int \mathcal{D}\bar{\psi}\mathcal{D}\psi \mathcal{D}M\mathcal{D}F\mathcal{D}\Delta^\dagger\mathcal{D}\Delta \\ &\quad \exp\left[i\int d^4x\left\{\bar{\psi}(i\gamma^\mu\partial_\mu - M)\psi - \bar{\psi}F\Sigma_z\tau_z\psi \right. \right. \\ &\quad \left. \left. - \frac{1}{2}\Delta^\dagger\bar{\psi}^C\gamma^5\tau_y\lambda_2\psi + \frac{1}{2}\Delta\bar{\psi}\gamma^5\tau_y\lambda_2\psi^C + \mu\bar{\psi}\gamma^0\psi \right. \right. \\ &\quad \left. \left. - \frac{M^2}{4G_S} - \frac{F^2}{2G_T} - \frac{|\Delta|^2}{2G_C}\right\}\right].\end{aligned}\quad (3)$$

In order to transform the above expression into bilinear form for quark fields, we decompose it into

$$\begin{aligned}
Z \propto & \int \mathcal{D}\bar{\psi}\mathcal{D}\psi \mathcal{D}M\mathcal{D}F\mathcal{D}\Delta^\dagger\mathcal{D}\Delta \\
& \exp \left[\frac{i}{2} \int d^4x \left\{ \bar{\psi}(i\gamma^\mu\partial_\mu - M)\psi - \bar{\psi}^C(i\gamma^\mu\overleftarrow{\partial}_\mu - M)\psi^C \right. \right. \\
& \quad - \bar{\psi}F\Sigma_z\tau_z\psi + \bar{\psi}^CF\Sigma_z\tau_z\psi^C \\
& \quad - \Delta^\dagger\bar{\psi}\gamma^5\tau_y\lambda_2\psi + \Delta\bar{\psi}\gamma^5\tau_y\lambda_2\psi^C \\
& \quad \left. \left. + \mu\bar{\psi}\gamma^0\psi - \mu\bar{\psi}^C\gamma^0\psi^C \right\} \right] \\
& \times \exp \left[-i \int d^4x \left\{ \frac{M^2}{4G_S} + \frac{F^2}{2G_T} + \frac{|\Delta|^2}{2G_C} \right\} \right].
\end{aligned}$$

Let us define the Nambu spinors:

$$\Psi(x) := \frac{1}{\sqrt{2}} \begin{pmatrix} \psi(x) \\ \psi^C(x) \end{pmatrix}, \quad \bar{\Psi}(x) := \frac{1}{\sqrt{2}} (\bar{\psi}(x) \quad \bar{\psi}^C(x)). \quad (4)$$

Using these spinors, we can rewrite the generating functional into bilinear form of quarks as follows:

$$\begin{aligned}
Z \propto & \int \mathcal{D}\bar{\Psi}\mathcal{D}\Psi \mathcal{D}M\mathcal{D}F\mathcal{D}\Delta^\dagger\mathcal{D}\Delta \\
& \exp \left[i \int d^4x \left\{ \bar{\Psi}(x)S^{-1}(x)\Psi(x) - \frac{M^2}{4G_S} - \frac{F^2}{2G_T} - \frac{|\Delta|^2}{2G_C} \right\} \right]. \quad (5)
\end{aligned}$$

Here we define the inverse propagator in position space:

$$S^{-1}(x) := \begin{pmatrix} s_{11} & s_{12} \\ s_{21} & s_{22} \end{pmatrix}, \quad (6)$$

and

$$\begin{aligned}
s_{11} &:= (i\gamma^\mu\partial_\mu - M + \mu\gamma^0)\mathbf{1}_F\mathbf{1}_C - F\Sigma_z\tau_z\mathbf{1}_C, \\
s_{12} &:= \Delta\gamma^5\tau_y\lambda_2, \\
s_{21} &:= -\Delta^\dagger\gamma^5\tau_y\lambda_2, \\
s_{22} &:= (-i\gamma^\mu\overleftarrow{\partial}_\mu - M - \mu\gamma^0)\mathbf{1}_F\mathbf{1}_C + F\Sigma_z\tau_z\mathbf{1}_C,
\end{aligned}$$

where $\mathbf{1}_F$ and $\mathbf{1}_C$ are the unit matrices for flavor space and color space, respectively. We can integrate Z with respect to $\bar{\psi}$ and ψ , then we obtain

$$\begin{aligned}
Z \propto & \int \mathcal{D}M\mathcal{D}F\mathcal{D}\Delta^\dagger\mathcal{D}\Delta \\
& \exp \left[\frac{1}{2} \log \text{Det } S^{-1}(x) - i \int d^4x \left\{ \frac{M^2}{4G_S} + \frac{F^2}{2G_T} + \frac{|\Delta|^2}{2G_C} \right\} \right],
\end{aligned}$$

where Det means functional determinant over position space, the Nambu space, gamma matrices, flavor and color space. To compute $\text{Det } S^{-1}(x)$ we move to momentum space. The generating functional in momentum

space becomes

$$\begin{aligned}
Z \propto & \int \mathcal{D}M\mathcal{D}F\mathcal{D}\Delta^\dagger\mathcal{D}\Delta \\
& \exp \left[\frac{1}{2} \int d^4p \int \frac{d^4p}{(2\pi)^4} \log \det \tilde{S}^{-1}(p) \right. \\
& \quad \left. - i \int d^4x \left\{ \frac{M^2}{4G_S} + \frac{F^2}{2G_T} + \frac{|\Delta|^2}{2G_C} \right\} \right], \quad (7)
\end{aligned}$$

where det is for the Nambu space, gamma matrices, flavor space and color space, and we introduce the inverse propagator in momentum space as follows:

$$\tilde{S}^{-1}(p) := \begin{pmatrix} \tilde{s}_{11} & \tilde{s}_{12} \\ \tilde{s}_{21} & \tilde{s}_{22} \end{pmatrix}, \quad (8)$$

where

$$\begin{aligned}
\tilde{s}_{11} &:= (\not{p} - M + \mu\gamma^0)\mathbf{1}_F\mathbf{1}_C - F\Sigma_z\tau_z\mathbf{1}_C, \\
\tilde{s}_{12} &:= \Delta\gamma^5\tau_y\lambda_2, \\
\tilde{s}_{21} &:= -\Delta^\dagger\gamma^5\tau_y\lambda_2, \\
\tilde{s}_{22} &:= (\not{p} - M - \mu\gamma^0)\mathbf{1}_F\mathbf{1}_C + F\Sigma_z\tau_z\mathbf{1}_C.
\end{aligned}$$

Calculating $\det \tilde{S}^{-1}(p) = 0$ for p_0 gives us single-particle energies for quasi-particles. Thus, for simplicity, we introduce two kinds of single-particle energies:

$$\varepsilon^{(\alpha,\beta)} := \sqrt{p_z^2 + \left(\sqrt{p_x^2 + p_y^2 + M^2 + \alpha F} \right)^2} + \beta\mu \quad (9)$$

$$E^{(\alpha,\beta)} := \sqrt{(\varepsilon^{(\alpha,\beta)})^2 + \Delta^2}, \quad (10)$$

where $\alpha = \pm$ and $\beta = \pm$.

After calculating $\det \tilde{S}^{-1}(p)$, we get

$$\begin{aligned}
& \log \det \tilde{S}^{-1}(p) \\
&= \log \left[\left\{ \prod_{\alpha,\beta=\pm} (p_0 - \varepsilon^{(\alpha,\beta)})(p_0 + \varepsilon^{(\alpha,\beta)}) \right\}^{N_F} \right. \\
& \quad \left. \times \left\{ \prod_{\alpha,\beta=\pm} (p_0 - E^{(\alpha,\beta)})(p_0 + E^{(\alpha,\beta)}) \right\}^{2N_F} \right],
\end{aligned}$$

where N_F means the number of flavor (in this case $N_F = 2$). In order to calculate the Matsubara summation later, we differentiate and integrate the above expression with respect to single-particle energies:

$$\begin{aligned}
& \log \det \tilde{S}^{-1}(p) \\
&= N_F \sum_{\alpha,\beta=\pm} \left\{ \int d\varepsilon^{(\alpha,\beta)} \left(\frac{1}{p_0 + \varepsilon^{(\alpha,\beta)}} - \frac{1}{p_0 - \varepsilon^{(\alpha,\beta)}} \right) \right. \\
& \quad \left. + 2 \int dE^{(\alpha,\beta)} \left(\frac{1}{p_0 + E^{(\alpha,\beta)}} - \frac{1}{p_0 - E^{(\alpha,\beta)}} \right) \right\}.
\end{aligned}$$

To discuss the system at finite temperature, we use the following substitution:

$$\int \frac{d^4p}{i(2\pi)^4} f(p_0, \vec{p}) \rightarrow T \sum_{n=-\infty}^{\infty} \int \frac{d^3p}{(2\pi)^3} f(i\omega_n, \vec{p}),$$

where T is temperature and $\omega_n := (2n+1)\pi T$, ($n \in \mathbb{Z}$) is the Matsubara frequency for fermion. Using this substitution, the component of the the generating functional becomes

$$\begin{aligned} & \frac{1}{2} \int \frac{d^4 p}{(2\pi)^4} \log \det \tilde{S}^{-1}(p) \\ & \rightarrow \frac{iT}{2} N_F \sum_{n=-\infty}^{\infty} \int \frac{d^3 p}{(2\pi)^3} \sum_{\alpha, \beta = \pm} \\ & \left\{ \int d\varepsilon^{(\alpha, \beta)} \left(\frac{1}{i\omega_n + \varepsilon^{(\alpha, \beta)}} - \frac{1}{i\omega_n - \varepsilon^{(\alpha, \beta)}} \right) \right. \\ & \quad \left. + 2 \int dE^{(\alpha, \beta)} \left(\frac{1}{i\omega_n + E^{(\alpha, \beta)}} - \frac{1}{i\omega_n - E^{(\alpha, \beta)}} \right) \right\}. \end{aligned}$$

We can calculate the Matsubara summation with the following formula:

$$\lim_{\eta \rightarrow +0} T \sum_{n=-\infty}^{\infty} \frac{e^{i\omega_n \eta}}{i\omega_n - x} = \lim_{\eta \rightarrow +0} \frac{e^{i\omega_n \eta}}{1 + e^{x/T}} = \frac{1}{1 + e^{x/T}}.$$

Using the above formula and integrating with respect to energies, the above expression becomes

$$\begin{aligned} & \frac{i}{2} N_F \int \frac{d^3 p}{(2\pi)^3} \sum_{\alpha, \beta} \left[\varepsilon^{(\alpha, \beta)} + 2T \log \left(1 + \exp[-\varepsilon^{(\alpha, \beta)}/T] \right) \right. \\ & \quad \left. + 2 \left\{ E^{(\alpha, \beta)} + 2T \log \left(1 + \exp[-E^{(\alpha, \beta)}/T] \right) \right\} \right] \\ & \quad + \text{const}, \end{aligned}$$

where “const” is a constant of integration¹. Since constant terms do not contribute to thermodynamics, we ignore them. Substituting the result into the generating functional, Z becomes

$$\begin{aligned} Z & \propto \int \mathcal{D}M \mathcal{D}F \mathcal{D}\Delta^\dagger \mathcal{D}\Delta \\ & \exp \left[iN_F \int d^4 x \int \frac{d^3 p}{(2\pi)^3} \sum_{\alpha, \beta} \left\{ \frac{\varepsilon^{(\alpha, \beta)}}{2} + E^{(\alpha, \beta)} \right. \right. \\ & \quad \left. \left. + T \log \left(1 + \exp[-\varepsilon^{(\alpha, \beta)}/T] \right) \left(1 + \exp[-E^{(\alpha, \beta)}/T] \right)^2 \right\} \right] \\ & \times \exp \left[-i \int d^4 x \left\{ \frac{M^2}{4G_S} + \frac{F^2}{2G_T} + \frac{|\Delta|^2}{2G_C} \right\} \right]. \end{aligned} \quad (11)$$

In one-loop approximation we obtain the thermodynamic

potential as follows:

$$\begin{aligned} V(M, F, |\Delta|, \mu, T) & = -N_F \int \frac{d^3 p}{(2\pi)^3} \sum_{\alpha, \beta} \left\{ \frac{\varepsilon^{(\alpha, \beta)}}{2} + E^{(\alpha, \beta)} \right. \\ & \quad \left. + T \log \left(1 + \exp[-\varepsilon^{(\alpha, \beta)}/T] \right) \left(1 + \exp[-E^{(\alpha, \beta)}/T] \right)^2 \right\} \\ & \quad + \frac{M^2}{4G_S} + \frac{F^2}{2G_T} + \frac{|\Delta|^2}{2G_C}. \end{aligned} \quad (12)$$

III. NUMERICAL RESULTS

In this section we calculate the thermodynamic potential numerically. To do this we use parameters in Table I. Since the NJL model is not a renormalizable theory, we adopt a three-momentum cutoff parameter, Λ .

A. Chiral condensate versus color superconducting gap

First we discuss the relationship between the chiral condensed phase and the color superconducting phase. We show numerical results of the thermodynamic potential in Fig 1. The horizontal and vertical axes represent the order parameters for the chiral condensate, M , and the color superconducting gap, Δ , respectively. Darker color represents lower value of the thermodynamic potential.

At chemical potential $\mu = 0.25$ GeV and temperature $T = 0.01, 0.08$ GeV, only the chiral condensed phase is realized. However, at $\mu = 0.25$ GeV and $T = 0.12$ GeV, both phases, the chiral condensed phase and the color superconducting phase, disappear.

At $\mu = 0.32$ GeV and $T = 0.01$ GeV, the chiral condensed phase exists and color superconducting gap does not appear. But there are two local minima on the horizontal and vertical axes, respectively. At $\mu = 0.32$ GeV and $T = 0.03$ GeV, there are also two local minima. The thermodynamic potential takes about the same value at these points. At $\mu = 0.32$ GeV and $T = 0.05$ GeV, there is no condensate.

On the other hand when $\mu = 0.35$ GeV and $T = 0.01$ GeV, the color superconducting phase appears but the chiral condensate disappears. At $\mu = 0.35$ GeV and $T = 0.02$ GeV, the color superconducting phase is the only phase realized. Like other cases, in high temperature

TABLE I. parameter set

Λ/GeV	G_S/GeV^{-2}	G_T/GeV^{-2}	G_C/GeV^{-2}
0.631	5.5	11.0	6.6

¹ Here we interchange $\sum_{n=-\infty}^{\infty}$ and $\int d^3 p$ to calculate the Matsubara summation. This interchange is not correct mathematically, however, the resulting generating functional is correct. This technique has been used in Ref.[25]

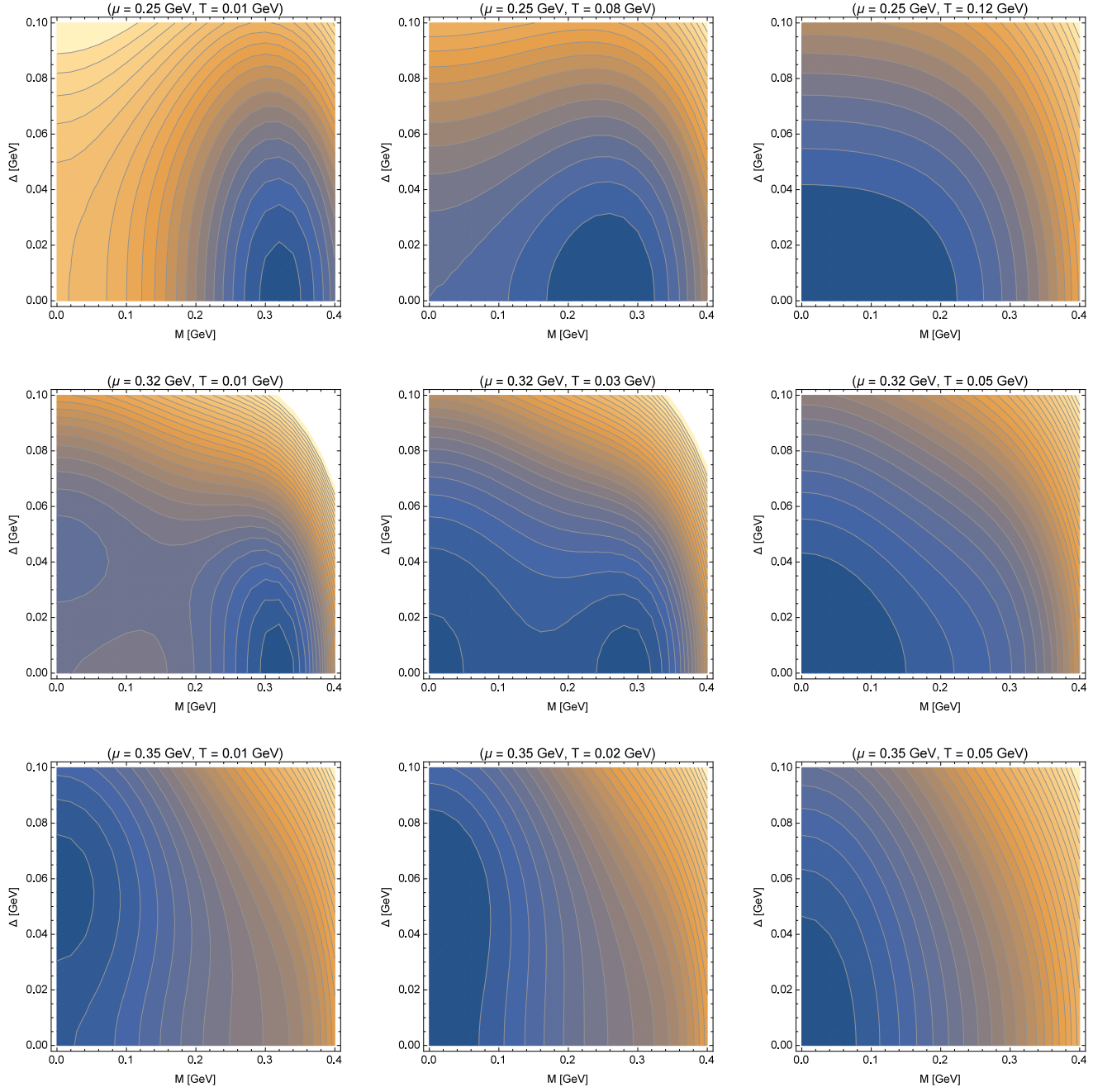


FIG. 1. The figures show the contour maps of the thermodynamic potential with several values of the chemical potential, μ and temperature, T . The horizontal and vertical axes represent the order parameters M and Δ for the chiral condensate and the color superconducting gap, respectively. Darker color represents lower values of the thermodynamic potential.

region ($\mu = 0.35$ GeV and $T = 0.05$ GeV), there is no condensate.

These contour plots indicate that the chiral condensed phase and the color superconducting phase do not coexist in our parameter set. In Ref. [19], however, it has been shown that if one adopts a different parameter set, the two phases may coexist.

It is known that there is an end point where the order of the phase transition between the chiral condensed phase

and chiral symmetric phase changes in the phase diagram in the T - μ plane. In the low chemical potential region, the phase transition is of second order, on the other hand, in large chemical potential region, it is of the first order.

According to the numerical results, if the chiral condensate is realized, the thermodynamic potential always takes the minimum value on the horizontal axes. On the other hand, if the color superconducting gap is realized, the thermodynamic potential always takes the minimum

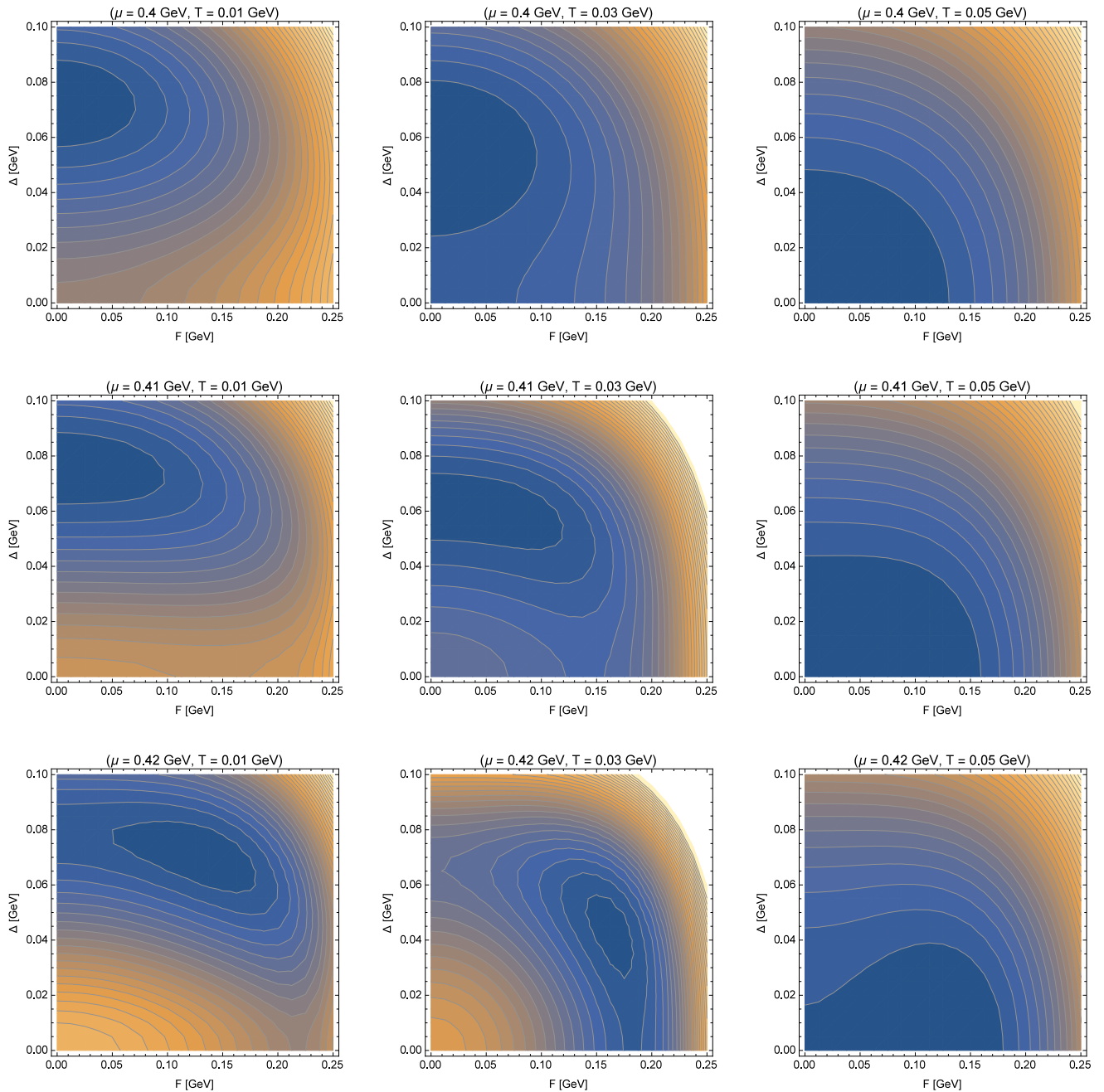


FIG. 2. The figures show the contour maps of the thermodynamic potential with several values of the chemical potential, μ and temperature, T . The horizontal and vertical axes represent the order parameters for the spin polarization and the color superconductivity, respectively. Darker color represents lower values of the thermodynamic potential.

value on the vertical axes. Thus, we consider that the order of the phase transition between the chiral condensed phase and the color superconducting phase is first order.

B. Spin polarization versus color superconductor

Next we discuss the relationship between the spin polarization and the color superconductivity. We plot the thermodynamic potential in Fig 2. The horizontal

and vertical axes represent the order parameter for the spin polarization and the color superconductivity, respectively. Darker color represents lower values of the thermodynamic potential.

At chemical potential $\mu = 0.4$ GeV and temperature $T = 0.01, 0.03$ GeV, the thermodynamic potential takes the minimum value at $F = 0$ and $\Delta \neq 0$. Thus the color superconducting phase is realized. At $\mu = 0.4$ GeV and $T = 0.05$ GeV, the thermodynamic potential takes the minimum value at the origin. It means that the simple

quark phase is realized.

At $\mu = 0.41$ GeV and $T = 0.01$ GeV, there is the only a color superconducting gap. However, at $\mu = 0.41$ GeV and $T = 0.03$ GeV, the thermodynamic potential takes the minimum value at $F \neq 0$ and $\Delta \neq 0$. It indicates that two phases may coexist. At $\mu = 0.41$ GeV and $T = 0.05$ GeV, both condensates disappear and the simple quark phase is realized.

At $\mu = 0.42$ GeV and $T = 0.01, 0.03$ GeV, the color superconducting gap and the spin polarized condensate coexist. Then, when $\mu = 0.42$ GeV and $T = 0.05$ GeV, the color superconducting gap disappears and the spin polarized condensate is realized. If we set higher temperatures, the thermodynamic potential will take the minimum at the origin, namely, no condensate appear.

According to these contour maps, we consider that the spin polarized phase and the color superconducting phase can coexist in certain conditions, and the order of the phase transition between the color superconducting phase, the spin polarized phase and the coexisting phase is of the second.

C. Phase diagram

Here we show the phase diagram in T - μ plane in Fig 3. The horizontal and vertical axes represent quark chemical potential and temperature, respectively.

The left region of the blue dotted and yellow solid lines, represents the chiral condensed phase. The blue dotted and yellow solid lines mean the second- and first-order phase transition between the chiral condensed phase and the chiral symmetrical phase, respectively.

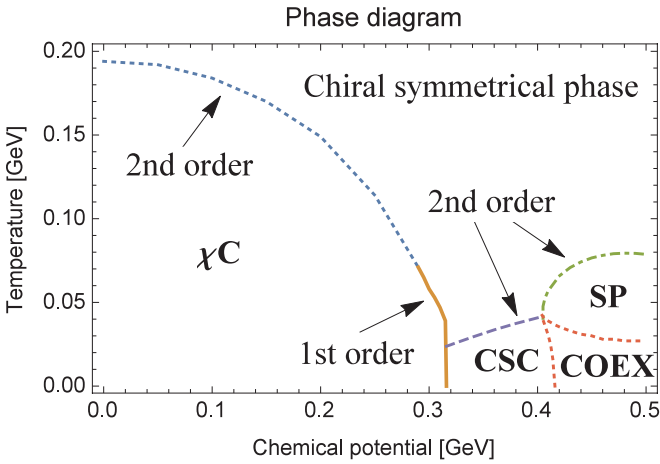


FIG. 3. The phase diagram with $G_T = 2G_S$: The horizontal and vertical axes represent chemical potential and temperature, respectively. In the figure, χC , CSC and SP mean the chiral condensed phase, the color superconducting phase and the spin polarized phase, respectively. Also, COEX means the coexisting phase with both the spin polarization and the color superconducting gap. “2nd order” and “1st order” mean the order of the phase transition.

The middle region below the violet dashed line is the color superconducting phase. The color superconducting phase can exist in the low temperature region, and, as chemical potential increases, the critical temperature for the phase transition between color superconducting and normal phase increases.

The right region of the orange dotted line is the coexisting phase where the color superconducting gap and the spin polarized condensate coexist. The critical temperature for the coexisting phase decreases as chemical potential increases. Note that just above the chemical potential $\mu = 0.4$ GeV and at low temperature the color superconducting phase exists, however, if we increase temperature slightly, we arrive at the coexisting phase. The region above the coexisting phase, namely, below green dash-dotted line, is a spin polarized phase.

D. Effect of the coupling constant G_T

Finally we investigate the effect of the coupling constant G_T on the thermodynamics. Here, we have used G_T as a free parameter. So we give the phase diagram with a new coupling constant: $G_T = 2.6G_S = 14.3 \text{ GeV}^{-2}$. Figure 4 shows the phase diagram with the new G_T in T - μ plane. One of the differences between the former phase diagram and the later one is that the color superconducting phase does not appear. Instead, the coexistence phase is realized after the chiral condensed phase disappears. Moreover, the spin polarized phase survives at higher temperatures, on the other hand, the coexisting phase disappears at lower temperatures than the former phase diagram.

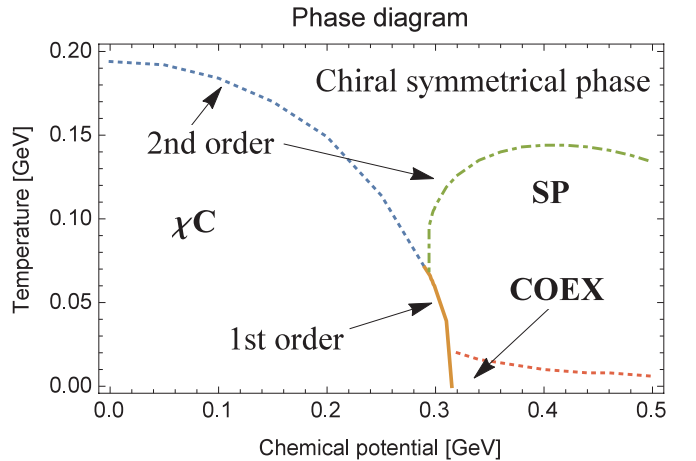


FIG. 4. The phase diagram with $G_T = 2.6G_S$: The horizontal and vertical axes represent chemical potential and temperature, respectively. In the figure, χC and SP mean the chiral condensed phase and spin polarized phase, respectively. Also, COEX means the coexisting phase with the spin polarization and color superconducting gap. “2nd order” and “1st order” mean the order of the phase transition.

IV. CONCLUSIONS AND REMARKS

We have studied the relationship between the chiral condensation, the color superconductivity and the spin polarization at finite density and temperature. According to the results, in the low chemical potential and temperature region, the chiral condensed phase exists and there is an end point where the order of the phase transition changes. In the intermediate chemical potential and low temperature region, the color superconducting phase exists. The chiral condensed and the color superconducting phases do not coexist in our parameter set, however, if we change values of the coupling strengths and/or three-momentum cutoff parameter, they may coexist. As is known well, the first order phase transition occurs from the chiral condensed phase to the color superconducting phase in the low temperature region. In large chemical potential and low temperature region, the color superconducting phase and the spin polarized phase coexist. However, if we increase temperature, the color superconductivity disappears soon and the only spin polarized phase is realized. The order of the phase transition between these phases is second order. At higher temperatures, there are no condensates. The extension of the spin polarization and color superconducting phase domains depends on the strength of the coupling of the tensor term.

Here we refer to the effect of the coupling constant, G_T , to the phase diagram. We have also examined several values of G_T : $G_T = 1.5G_S$, $1.75G_S$, $1.8G_S$, $3G_S$ and $3.5G_S$. When $G_T = 1.5G_S$, we obtain neither the spin polarized phase nor the coexistence phase. Thus, if we want these phases to be realized, the value of G_T must be larger than $1.5G_S$. When $G_T = 1.75G_S$ and $1.8G_S$, we can get phase diagrams qualitatively identical to one for $G_T = 2G_S$ (see Fig 3). When $G_T = 3G_S$, we obtain a phase diagram qualitatively identical to $G_T = 2.6G_S$ (see Fig 4). If $G_T = 3.5G_S$, the spin polarized phase is realized at $\mu = 0$, therefore, we consider that the value is too large.

In this paper we have considered the Lagrangian density with flavor $SU(2)$ and color $SU(3)$ symmetry. However, at large chemical potential, we should not ignore contributions from strange-quark. So, our next task is to consider the Lagrangian density with flavor $SU(3)$ symmetry. In this case a CFL phase may exist. It is also interesting to consider effects from an external magnetic field on the spin polarization, although effects from magnetic fields on the QCD phase diagram have been investi-

gated by many researchers [20, 21]. Moreover, in order to describe compact stars, we should consider charge neutrality and β -equilibrium. In the present work we have considered $\mu_u = \mu_d = \mu$, where μ_u and μ_d are chemical potentials for up- and down-quarks, respectively, and no charge neutrality. This will be considered in future works.

ACKNOWLEDGEMENTS

One of the authors (Y.T.) is partially supported by the Grants-in-Aid of the Scientific Research (No.26400277) from the Ministry of Education, Culture, Sports, Science and Technology in Japan.

Appendix A: Brief note for charge conjugate matrix and Dirac matrices

In section II we transform the Lagrangian density into bilinear form for the quark fields. Here we show how we can do it. We use gamma matrices represented by Dirac representation. Charge conjugate is define by

$$\bar{\psi}^C := \psi^T C, \quad \psi^C := C \bar{\psi}^T, \quad (A1)$$

where charge conjugate matrix is $C := i\gamma^0\gamma^2$. We enumerate properties of C matrix and gamma matrices:

$$C^\dagger = -C, \quad C^2 = -1,$$

and

$$(\gamma^0)^T = \gamma^0, \quad (\gamma^1)^T = -\gamma^1, \quad (\gamma^2)^T = \gamma^2, \quad (\gamma^3)^T = -\gamma^3.$$

When C matrix operates on gamma matrices, we obtain

$$C\gamma^0C = \gamma^0, \quad C\gamma^1C = -\gamma^1, \quad C\gamma^2C = \gamma^2, \quad C\gamma^3C = -\gamma^3.$$

Using these properties, we can get the following expressions:

$$\bar{\psi}^C \psi^C = \bar{\psi} \psi, \quad (A2)$$

$$\bar{\psi}^C \gamma^0 \psi^C = -\bar{\psi} \gamma^0 \psi \quad (A3)$$

$$\bar{\psi}^C \overleftarrow{\partial}_\mu \gamma^\mu \psi^C = -\bar{\psi} \gamma^\mu \partial_\mu \psi, \quad (A4)$$

$$\bar{\psi}^C \gamma^1 \gamma^2 \psi^C = -\bar{\psi} \gamma^1 \gamma^2 \psi, \quad (A5)$$

where last line means $\bar{\psi}^C \Sigma_z \psi^C = -\bar{\psi} \Sigma_z \psi$.

-
- [1] Y. Nambu and G. Jona-Lasinio, Phys. Rev **122**, 345 (1961).
 - [2] Y. Nambu and G. Jona-Lasinio, Phys. Rev **124**, 246 (1961).
 - [3] M. Alford, Ann. Rev. Nucl. Part. Sci, **51**, 131 (2001).

- [4] M. Buballa and M. Oertel, Nucl. Phys. A, **703**, 770 (2002).
- [5] M. Buballa, Phys. Rep. **407**, 205 (2005).
- [6] A. K. Harding and D. Lai, Rept. Prog. Phys. **69**, 2631 (2006).
- [7] T. Tatsumi, Phys. Lett. B, **489**, 280 (2000).

- [8] T. Tatsumi, T. Maruyama and E. Nakano, arXiv:0312351.
- [9] T. Tatsumi, T. Maruyama and E. Nakano, Prog. Theor. Phys. Suppl. No. 153, 190 (2004)
- [10] E. Nakano, T. Maruyama and T. Tatsumi, Phys. Rev. D **68**, 105001 (2003).
- [11] S. Maedan, Prog. Theor. Phys, **118**, 729 (2007).
- [12] M. Kitazawa, T. Koide, T. Kunihiro, and Y. Nemoto, Prog. Theor. Phys, **108**, 929 (2002).
- [13] H. Bohr, P. K. Panda, C. Providência and J. da Providência, Int. J. Mod. Phys. E **22**, 1350019 (2013).
- [14] E. J. Ferrer, V. de la Incera, I. Portillo, and M. Quiroz, Phys. Rev. D **89**, 085034 (2014).
- [15] Y. Tsue, J. da Providência, C. Providência, M. Yamamura, and H. Bohr, Prog. Theor. Exp. Phys. **2013**, 103D01 (2013).
- [16] Y. Tsue, J. da Providência, C. Providência, M. Yamamura, and H. Bohr, Prog. Theor. Exp. Phys. **2015**, 103D01 (2015).
- [17] H. Matsuoka, Y. Tsue, J. da Providência, C. Providência, M. Yasumura, and H. Bohr, Prog. Theor. Exp. Phys. **2016**, 053D02 (2016).
- [18] Y. Tsue, J. da Providência, C. Providência, M. Yamamura, and H. Bohr, Prog. Theor. Exp. Phys. **2015**, 103D01 (2015).
- [19] D. Blaschke, M. K. Volkov, and V. L. Yudichev, Eur. Phys. J. A **17**, 103 (2003).
- [20] J. O. Andersen and W. R. Naylor, Rev. Mod. Phys, **88**, 025001.
- [21] D. P. Menezes, M. B. Pinto, S. S. Avancini, A. P. Martínez and C. Providência, Phys. Rev. C **79**, 035807 (2009).
- [22] S. P. Klevansky, Rev. Mod. Phys, **64**, No. 3, 649 (1992).
- [23] T. Hatsuda and T. Kunihiro, Phys. Rep. **247**, 221 (1994).
- [24] Y. Tsue, J. da Providência, C. Providência, and M. Yamamura, Prog. Theor. Phys, **128**, 507 (2012).
- [25] M. Le Bellac, *Thermal Field Theory* (Cambridge University Press, Cambridge, England, 1996).